Research Article *Science, Engineering and Health Studies 2020, 14(1), 47-61*

Investigation of various factors affecting methylene blue adsorption on agricultural waste: Banana stalks

Jongporn Mahadlek[1*] and Jongjan Mahadlek[2]

[1]*Department of Environmental Science, Faculty of Science and Technology, Rajabhat Rajanagarindra University, Chachoengsao 24000, Thailand*
[2]*Pharmaceutical Intellectual Center Prachote Plengwittaya, Faculty of Pharmacy, Silpakorn University, Nakhon Pathom 73000, Thailand*
[*]*Corresponding author: jongporn.mah@mail.rru.ac.th*

Received: October 4, 2019; Revised: April 28, 2020; Accepted: April 28, 2020

ABSTRACT

Banana stalks are interesting agricultural waste products that can be utilized to eliminate dyes from textile wastewater because it is a low cost adsorbent and a readily available resource in Thailand. This study investigated the effect of various factors on methylene blue (MB) adsorption on different sizes of dried banana stalks. Before and after MB adsorption, banana stalks were characterized using Fourier transform infrared spectroscopy, scanning electron microscopy, and powder X-ray diffraction. The factors that were investigated included adsorbent amount, contact time, shaking speed, and initial MB dye concentration. The adsorption profile was identified using the Langmuir and Freundlich isotherms. Results indicated that all factors affected the MB adsorption of banana stalks. The highest MB adsorption percentage was observed in banana stalks ranging in size from 0.18 mm to 0.25 mm (40-60 mesh (S)), followed by those ranging in size from 0.25 mm to 0.40 mm (60-80 mesh (M)) and from 1.0 cm to 1.5 cm. The equilibrium data of these three sizes of banana stalks fitted well to the Freundlich model. These results confirmed that the adsorption profile was multilayered and occurred through physicochemical interactions. The most suitable adsorption kinetics model was the pseudo-second-order kinetics model. Therefore, these data can be used as a reference in establishing an alternative method for removing various dyes from wastewater using low cost eco-friendly agricultural waste.

***Keywords*:** banana stalks; adsorption; methylene blue; adsorption isotherms; agricultural waste

1. INTRODUCTION

Currently, Thailand is internationally known as one of the top producers of fabrics and silks and has experienced substantial economic growth in the textile industry. However, serious environmental problems arise from the textile industry, such as water being polluted by untreated effluents. Aquatic plants are affected by dyes, which reduce the transmission of sunlight in water and induce toxic substances. Such toxic substances adversely affect not only aquatic life but also human health (Salleh et al., 2011). Hence, more attention has been focused on eliminating effluents and the potential toxicity and visibility problems that they cause. Therefore, wastewater from dyes needs to be treated prior to being discharged to the environment (Manna et al., 2017).

A number of industries use dyes in the manufacture of textiles, leather, rubber, plastics, and

cosmetics, thereby generating colored wastewater (Mittal et al., 2010). Dyes are categorized into three groups, namely, cationic, anionic, and nonionic (Amel et al., 2012). Methylene blue (MB) is a thiazide cationic dye that is widely used to dye fabrics, leather, paper, cotton, wool, and analytical reagents (Pandey and Ravi 2019; Greluk and Hubicki, 2011). Several studies have reported that MB causes vomiting, increased heart rate, shock, and tissue necrosis (Vadivelan and Kumar, 2005). The chemical structure of MB is shown in Figure 1.

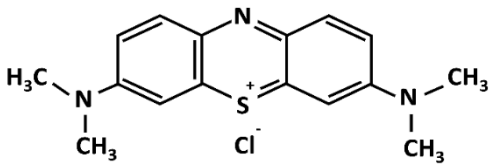

Figure 1 Chemical structure of methylene blue (MB; $C_{16}H_{18}N_3SCl$)

Many methods, such as physical methods (i.e., filtration, adsorption, ion exchange, and coagulation/ flocculation methods), chemical methods (i.e., Fenton reaction, ionization, and photocatalytic methods), and biological methods (i.e., aerobic and anaerobic degradation methods), have been adopted for the elimination of dyes from textile wastewater (Manna et al., 2017; Vital et al., 2016; Sulak et al., 2007; Xie et al., 2011). However, several techniques have limitations, such as sludge generation, formation of by-products, regeneration difficulties, ineffectiveness for all dyes, and high costs (Foo and Hameed, 2010). Previous studies have shown that adsorption is the most effective and economically feasible method among all available dye removal methods (Vital et al., 2016; Banerjee and Chattopadhyaya, 2017). Adsorption is extensively used as a separation procedure for removing dyes from industrial wastewaters. The dissolved components in a solution are attracted to the surface of solid materials (Bello et al., 2013).

Research on the use of adsorption materials (i.e., adsorbents) to remove dyes from wastewater has been conducted. Agricultural wastes, including rice husk, rice straw, coconut shell, sawdust, fly ash, tannin-rich materials, chitosan, seaweed and algae, pomelo peel, banana peel, mango peel, peat, and wood, have been utilized for dye adsorption (Vital et al., 2016). Waste from agricultural industries has an advantage because of its low cost and availability. The basic components of agricultural wastes, which include hemicellulose, lignin, and cellulose, indicate its potential sorption capacity for various pollutants (Demirbas, 2009).

The banana, Hom Thong variety (*Musa acuminata*) is an industrial crop, which is exported from Banlad, Phetchaburi province, Thailand to Japan (Nujnetra and Boonarong, 2013). Banana stalk is the part of the banana tree that usually becomes agricultural waste. Therefore, the banana stalk is an interesting adsorbent for dye removal from wastewater because of its low cost and positive impact on the agricultural waste problem. The banana stalk has a high cellulose content (i.e., 44% hemicellulose and only 8% lignin) (Shimizu et al., 2018). The particle size of banana peel powder is < 80 µm, which enables maximum MB adsorption (Moubarak et al., 2014).

A previous study focused on the sorption equilibrium and kinetics of MB dye from aqueous solution using banana stalk waste in Malaysia (Hameed et al., 2008). The banana stalk reached its adsorption equilibrium in 3.30 h for initial concentrations of 50-100 mg/L and equilibrium time of 4.30 h for initial concentrations of 200-500 mg/L. The Langmuir isotherm exhibited the best correlation for the sorption of MB on banana stalk. The maximum monolayer adsorption capacity of banana stalk (0.5-1 mm) was 243.90 mg/g at 30°C. However, the banana stalk was only used in the range of 0.5-1 mm. Therefore, the effect on the adsorbent size was a significant advantage in selecting the adsorbent size for further study. This research selected three adsorbent sizes, namely, 0.18-0.25 mm (40-60

mesh), 0.25-0.40 mm (60-80 mesh), and 1-2 cm. The purpose of this investigation was to explore the effect of critical parameters, which consist of the adsorbent amount, contact time, shaking speed, and initial MB dye concentration, on the adsorption capacity for MB in solution using different sizes of dried banana stalks as an adsorbent.

2. MATERIALS AND METHODS

2.1 Materials

Banana stalk, obtained from the Hom Thong variety (*M. acuminata*), is an agricultural waste from Banlad, Phetchaburi, Thailand. MB (C16H18N3CIS·2H2O, C.I. 52015, 82%, 355.89 g/mol; Ajax Finechem Pty Ltd, Australia) was used as a cationic dye model.

2.2 Preparation of the adsorbents

Banana stalks were washed, cut, and dried in sunlight for 3 days. Afterward, the samples were dried in a hot air oven (Binder, Scientific Promotion Co. Ltd., Thailand) at 50°C for 72 h. The dried banana stalks were milled and sifted through a 40-60 mesh (S), 60-80 mesh (M) and 1-1.5 cm (L). The different sizes of banana stalks are presented in Figure 2.

2.3 Preparation of the dye solution

Stock solutions were obtained by dissolving MB in distilled water. The stock solutions were then diluted to obtain the desired dye concentration (i.e., 50-200 mg/L). A calibration curve was developed to plot the adsorption data obtained using a UV-Vis spectrophotometer (Agilent 8453E, USA) at 665 nm (Carvalho et al., 2015).

2.4 Characterization of the adsorbent

2.4.1 Fourier transform infrared spectroscopy

Dried banana stalk was mixed with potassium bromide (1:100). The surface morphology of the adsorbent was observed by Fourier transform infrared spectroscopy (FTIR; Nicolet 6700 FTIR spectrometer, Thermo Fisher Scientific, USA) within the range of 400-4,000 cm^{-1} and the resolution of 4 cm^{-1}. The adsorbent functional groups that attributed to the binding of adsorbate molecules were identified (Salman et al., 2011).

2.4.2 Scanning electron microscopy and powder X-ray diffraction

The surface morphology of the adsorbent was visualized and evaluated using scanning electron microscopy (SEM; MIRA3, TESCAN USA, Inc., USA). The banana stalk surface was coated with thin gold and photographed before and after MB adsorption. The powder X-ray diffraction (XRD) technique was used for structural analysis using a powder X-ray diffractometer (Rigaku MiniFlex II, Rigaku Americas Corporation, USA) within the range of $2\theta = 5°$ to 45° with the scanning speed of 5°/min at room temperature.

Figure 2 Banana stalks: S, 40-60 mesh (A); M, 60-80 mesh (B); and L, 1-2 cm (C)

2.5 Adsorption equilibrium studies

The adsorption equilibrium of banana stalks was determined. Banana stalks were poured into 125 mL Erlenmeyer flasks with 50 mL of different initial MB dye concentrations within the range of 50-200 mg/L. The solution was agitated at 100 rpm for 60 min. The initial MB dye concentration at the equilibrium stage was quantified using a UV-Vis spectrophotometer at 665 nm. The temperature was controlled at 28°C during the adsorption process. The dye concentrations were calculated from the calibration curve. The experiments were evaluated three times. The amount of adsorbed MB dye and the MB adsorption percentage at the equilibrium stage was estimated using the following equations:

$$q_e = (C_0 - C_e)\,V/W, \quad (1)$$

$$\% \text{ adsorption} = (C_0 - C_e)/C_0 \times 100, \quad (2)$$

where C_0 (mg/L) is the MB concentration at the initial stage of the solution before adsorption, C_e (mg/L) is the MB concentration at the equilibrium stage of the solution after adsorption, V (L) is the volume of solution used, and W (g) is the mass of adsorbent.

The adsorption isotherms of MB on banana stalks were investigated with the initial MB dye concentrations of 50-200 mg/L. Two adsorption isotherms, namely, the Langmuir and Freundlich models, are widely used to explain the adsorption data. The Langmuir isotherm describes a homogeneous monolayer adsorption surface in which all sites are saturated; thus, adsorption is no longer possible (Sharma et al., 2018). The Langmuir model is expressed as follows (Hameed et al., 2008; Langmuir, 1918):

$$C_e/q_e = 1/K_L q_m + C_e/q_m, \quad (3)$$

where q_e (mg/g) is the amount of adsorbed MB dye per unit mass of adsorbent at the equilibrium stage, q_m (mg/g) is the maximum monolayer adsorption capacity of the adsorbent, and K_L (L/mg) is the Langmuir constant. The plot of C_e/q_e versus C_e showed a linear graph with slope and intercept as $1/q_m$ and $1/K_L q_m$, respectively. The favorability of the adsorption process (R_L) is calculated using the following equation (Hameed et al., 2008):

$$R_L = 1/(1 + K_L C_0), \quad (4)$$

The R_L values describe the behavior of adsorption to be an irreversible process ($R_L = 0$), a favorable process ($0 < R_L < 1$), and an unfavorable process ($R_L > 1$).

The Freundlich isotherm describes multilayer or heterogeneous adsorption in terms of the variation of adsorption sites (Zhang et al., 2016). The Freundlich model is expressed as follows (Hameed et al., 2008):

$$\log q_e = \log K_F + 1/n(\log C_e), \quad (5)$$

where K_F (mg/g) is the Freundlich constant of adsorption capability, and n is the adsorption intensity. The plot of $\log q_e$ versus $\log C_e$ showed a straight line with slope and intercept as 1/n and $\log K_F$, respectively. The favorability of adsorption was illustrated by the magnitude of the exponent (1/n).

2.6 Factors affecting MB adsorption on various sizes of banana stalks

The effect of adsorbent amount was evaluated by agitating 0.1-0.5 g adsorbent, and the initial MB dye concentration of 150 mg/L (50 mL) at a speed of 100 rpm for 60 min. The effect of contact time was evaluated using the optimized amount of adsorbent in the initial MB dye concentration of 150 mg/L (50 mL) and a shaking speed of 100 rpm for 30-120 min. The effect of shaking speed was investigated by adding the optimized amount of adsorbent in the initial MB dye concentration of 150 mg/L (50 mL) at various shaking speeds (i.e., 0 - 200 rpm) for 60 min.

2.7 Statistical analysis

All statistical analyzes were performed using SPSS version 16.0 software. The $p < 0.05$ was considered a significant difference. Duncan's multiple range test was selected for post hoc test (multiple comparison test).

3. RESULTS AND DISCUSSION

3.1 FTIR, SEM, and XRD of banana stalks

The surfaces of banana stalk functional groups before and after MB adsorption were investigated by FTIR. The spectra are displayed in Figure 3. The adsorption bands at 3,406, 2,924, 1,637, and 1,325 cm^{-1} were observed in the spectra corresponding to O-H stretching of hydroxyl groups (a broad peak) in cellulose and lignin, C-H stretching of methylene and methyl groups, C=H stretching vibration of conjugated groups in phenolic compound, and in-plane C-H bending and conjugated C-O stretching, respectively. Angular deformation of C-H linkages of aromatic groups was observed at 576 cm^{-1}. Cellulose, hemicellulose, and lignin were detected from the samples with aromatic amine, alkyne, and various oxygen functional groups. The results indicated the similarity between the compositions of banana fibers and other species. Notably, the banana stalk has functional groups that can interact with metallic ions and the biosorbent (Becker et al., 2013). The functional groups on the surface of the adsorbent consisting of -OH, -COOH, and -C=O denote the adsorbent's active sites that interact with the adsorbate dye solution (Zhao et al., 2017). The peak of MB at 3,422 cm^{-1} represents the OH group, which can be attributed to the presence of moisture in MB. The sharp band of MB at 1,599 cm^{-1} represents the C=N group, and the band between 1,179 cm^{-1} and 1,142 cm^{-1} represents the N-C bond of the aromatic amine functional groups. After MB adsorption, the adsorption peaks at 1,603 and 1,052-1,159 cm^{-1} were intense because of the overlapping of the C=N and N-C bonds from the aromatic amine functional groups in the cellulose or lignin structure of the banana stalk. The absorption peaks changed from 3,406, 2,924, and 1,325 cm^{-1} to 3,422, 2,921, and 1,329 cm^{-1}, respectively. This finding indicated that the MB molecules interacted with the adsorbent functional groups (Pathania et al., 2017). The active sites of banana stalk could attach to the MB molecules because of the strong electrostatic interaction between them. The positive charge of the MB molecule interacted with the negative charge of the banana stalk. However, as previously reported, the negatively charged functional groups on the surface of the adsorbent (such as -CN-, -O-S-, and -COO-) interacted with the positively charged functional group of MB at $=N^{+}(CH_3)_2$, and MB adsorption occurred as multilayer adsorption with a pseudo-second-order kinetics model (Danish et al., 2018). The formation of a hydrogen bond between nitrogen atoms of MB and hydroxyl groups on the banana stalk surface (cellulose) and the electrostatic attraction between MB and banana stalk surface are shown in Figure 4 (Mohammad et al., 2010).

The banana stalk surface was observed using SEM. The surface morphology of banana stalk before MB adsorption is shown in Figure 5. The banana stalk pores were highly heterogeneous. After MB adsorption, the structure of the banana stalk showed a smooth surface because MB molecules covered the banana stalk surface.

The XRD spectra of the banana stalk before and after MB adsorption are presented in Figure 6. The structure of the banana stalk was cellulose based. The results showed that the peak at 2θ of 22° represented the cellulose structure and the peak at 2θ of 16° represented the polysaccharide structure (Liu et al., 2005). Sharp peaks indicating high crystallinity were observed before and after MB adsorption.

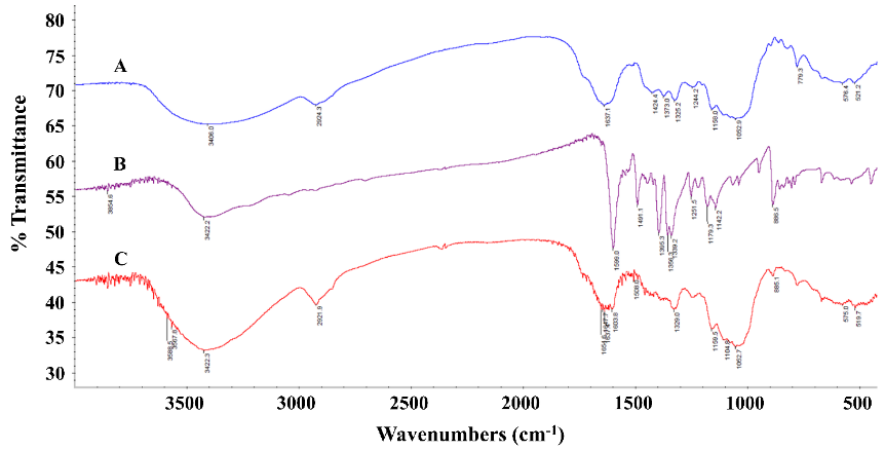

Figure 3 FTIR spectra of banana stalks before (A), after (C) MB adsorption, and MB (B)

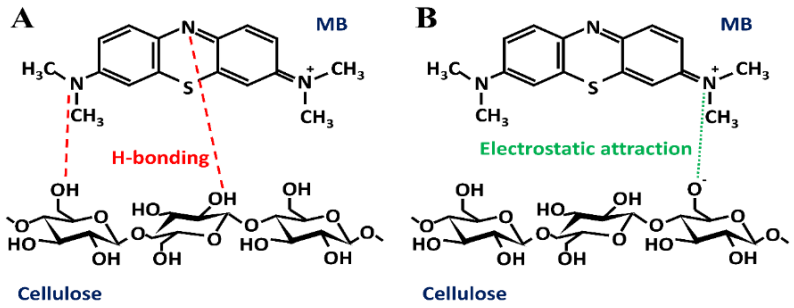

Figure 4 Schematic representation of the hydrogen bond (A) and electrostatic attraction (B) between MB and banana stalk cellulose (Mohammad et al., 2010)

3.2 Effect of adsorbent amount

The adsorbent amount was a significant factor in determining adsorption efficiency. The MB adsorption percentages were evaluated with various adsorbent amounts (i.e., 0.1-0.5 g) at the initial concentration of 150 mg/L, shaking speed of 100 rpm, and contact time of 60 min, as shown in Figure 7A. The MB adsorption percentage of banana stalk (S), (M), and (L) significantly increased ($p < 0.05$) from 36.4% to 84.0%, from 23.0% to 81.1%, and from 14.1% to 57.7% with the increase in the amount of banana stalk from 0.1 g to 0.3 g, from 0.1 g to 0.4 g, and from 0.1 g to 0.4 g, respectively. The equilibrium constant of MB adsorption was ultimately reached. Notably, banana stalk (S) showed the highest MB adsorption percentage; thus, 0.3 g was selected as the amount of banana stalk for further studies because the result of the 0.3-0.5 g adsorbent did not show a significant difference from the small banana stalks. Furthermore, these results indicated that the MB adsorption percentage significantly increased with the decrease in the adsorbent size ($p < 0.05$). The higher the adsorbent amount and surface area are, the larger the number of available adsorption sites. These findings could be associated with the banana stalk surface, as presented in Figure 5. The adsorption capability was elevated because the adsorbent surface had more available active sites (Singh et al., 2018). By contrast, the adsorption capacity remained

constant because of the saturation of the surface (Mouni et al., 2018). However, several studies have reported that adsorption on the surface area of the adsorbent decreased because increasing the adsorbent amount could lead to aggregation and unsaturation of adsorption sites (Mahmoodi, 2011; Yagub et al., 2014).

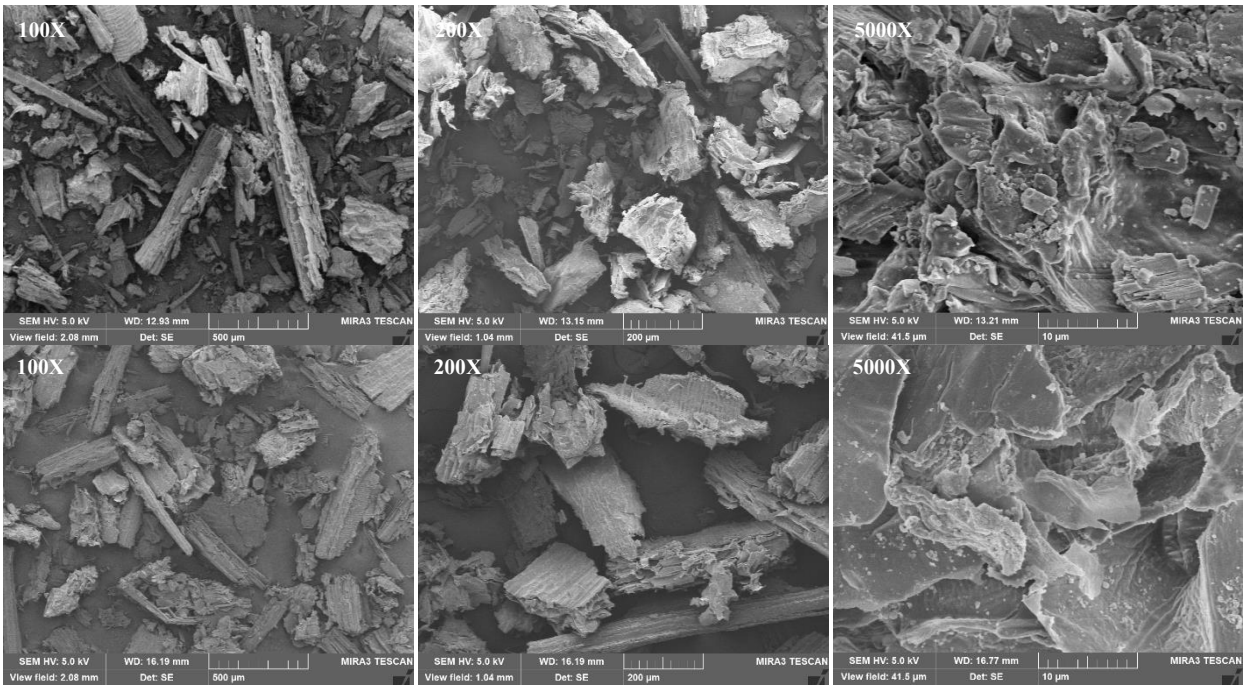

Figure 5 SEM photographs of banana stalk before (top row) and after (bottom row) MB adsorption at ×100, ×200, and ×5,000

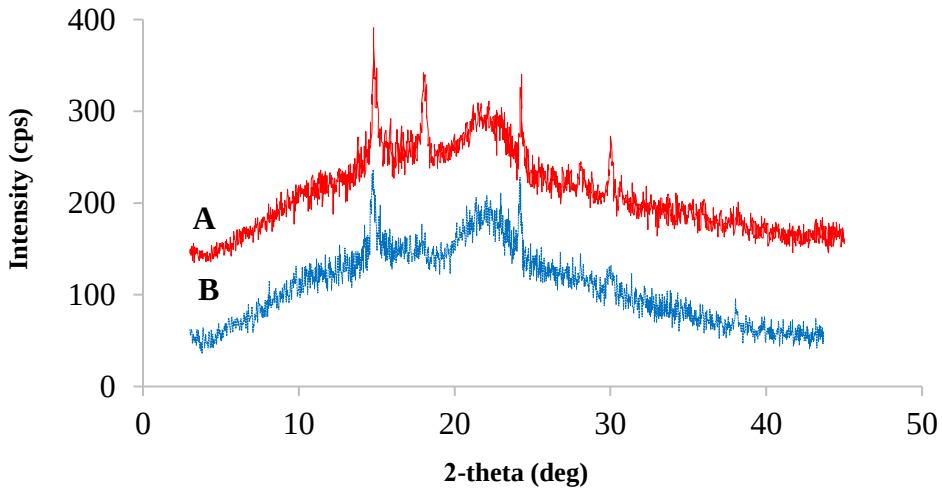

Figure 6 XRD patterns of banana stalk before (A) and after (B) MB adsorption

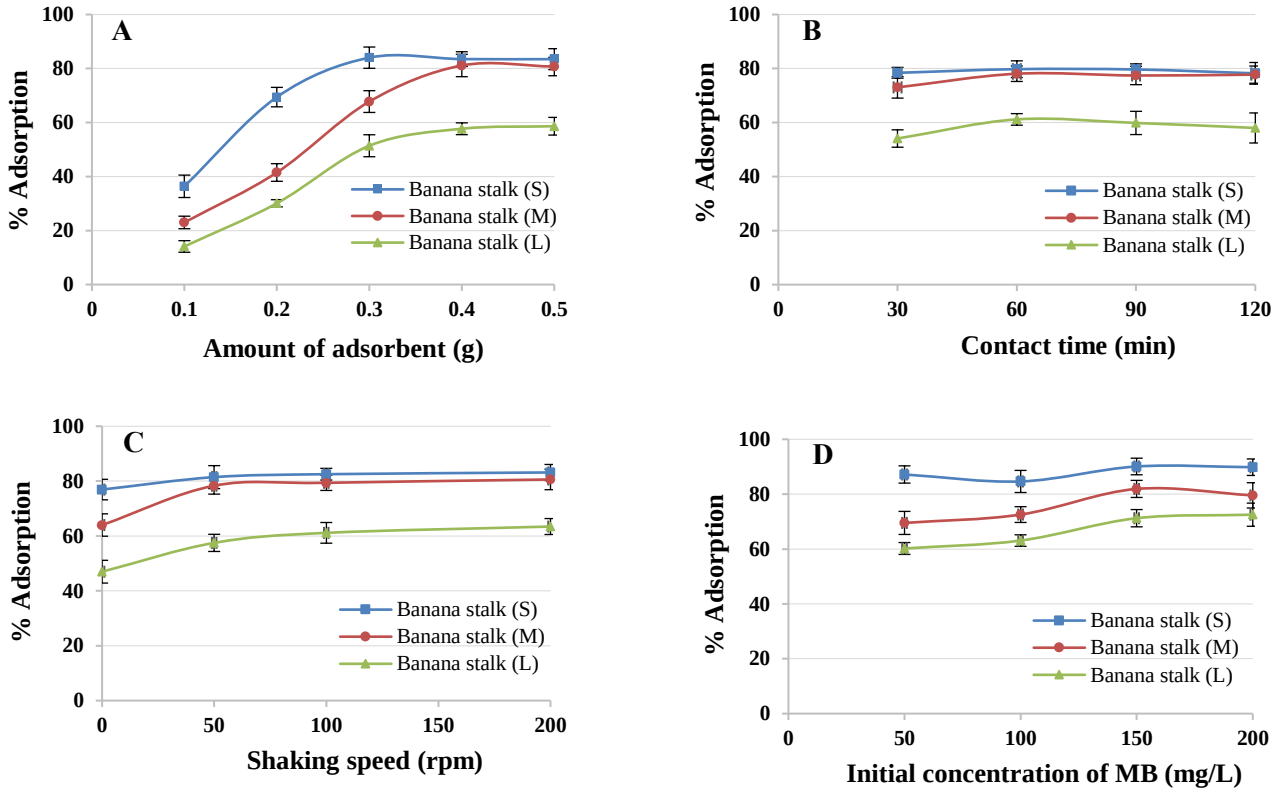

Figure 7 Effect of adsorbent amount (A), contact time (B), shaking speed (C), and initial MB dye concentration (D) on MB adsorption using various sizes of banana stalks

3.3 Effect of contact time

MB adsorption was evaluated using 0.3 g of banana stalks with the initial MB dye concentration of 150 mg/L at the shaking speed of 100 rpm. The effect of contact time on MB adsorption percentage with various sizes of banana stalks was determined, as shown in Figure 7B. MB adsorption of banana stalks (S), (M), and (L) reached its equilibrium within 60 min as 79.8%, 78.1%, and 61.2%, respectively. The statistical analysis showed that the effect of contact time on MB adsorption percentage of each size of banana stalk was not significantly different ($p > 0.05$). With the contact time of 30 min, the MB adsorption of banana stalk significantly increased with the decrease in the size of banana stalk ($p < 0.05$). The MB adsorption of banana stalks (S) and (M) was significantly higher than that of banana stalk (L) with the contact time between 60 min and 120 min ($p < 0.05$). Therefore, the contact time of 60 min was selected for further experiments.

3.4 Effect of shaking speed

The effect of shaking speed on MB adsorption of banana stalk was determined, as shown in Figure 7C. The MB adsorption percentage of banana stalks (M) and (L) with shaking was significantly higher than that without shaking ($p < 0.05$). Meanwhile, the effect of shaking speed on MB adsorption of banana stalk (S) was not significantly different ($p > 0.05$). The MB adsorption percentage of banana stalks (S), (M), and (L) at 100 rpm was 82.5%, 79.4%, and 63.5%, respectively. However, no significant difference was

observed when the shaking speed was between 50 rpm and 200 rpm ($p > 0.05$). Thus, the shaking speed of 100 rpm was used to further optimize the experiments. Shaking speed affected MB adsorption percentage because of the close contact between sorbent surface and adsorbate.

3.5 Effect of initial MB dye concentration

The effect of initial MB dye concentration on MB adsorption when using various sizes of banana stalks was evaluated at initial concentrations of 50-200 mg/L, as displayed in Figure 7D. The smaller banana stalk (S) had a significantly higher MB adsorption than the larger banana stalks (M and L) ($p < 0.05$). The MB adsorption of banana stalks (M) and (L) increased significantly with the increase in the initial MB dye concentration from 50 mg/L to 150 mg/L ($p < 0.05$). Meanwhile, with the increase in the initial MB dye concentration from 50 mg/L to 200 mg/L, the MB adsorption of banana stalk (S) showed no significant difference ($p > 0.05$). The optimum initial concentration of MB adsorption of 150 mg/L was selected for all sizes of banana stalks. A previous study reported that the MB adsorption of banana stalk increased with the increase in the adsorbent amount on the free active sites (Amel et al., 2012). At an initially high dye concentration, the mass transfer's strong driving force resulted in the increase in the adsorbent's capacity (Bulut and Aydin, 2006).

3.6 Adsorption equilibrium and adsorption isotherms

The MB adsorption profile of various sizes of banana stalks is shown in Figure 8. The concentration range of 0-200 mg/L presented a linear behavior. MB adsorption on banana stalks increased with the increase in the initial concentration of MB and the decrease in the adsorbent amount. The results revealed that the highest MB adsorption of banana stalks (S), (M), and (L) at the initial MB dye concentration of 150 mg/L was 90.1%, 81.9%, and 71.2%, respectively. The equilibrium MB adsorption profile of banana stalks was determined using the Langmuir and Freundlich models. The Langmuir isotherm described the saturated monolayer of dye molecules on the homogenous surface of the adsorbent at maximum adsorption. The Langmuir isotherm of MB adsorption on three sizes of banana stalks are shown in Figure 9.

The Langmuir constant (K_F) and the adsorption amount relative to the monolayer (q_m) were determined, as presented in Table 1. The q_m values of banana stalks (S) and (M) were 322.58 and 312.50 mg/g, respectively, indicating better adsorption capacity for MB than banana stalk (L) (250.00 mg/g). This finding indicated that the adsorption performance of small banana stalks was higher than that of large banana stalks. The R_L value of banana stalks (S), (M), and (L) was between 0.0094 and 0.0364, between 0.0092 and 0.0357, and between 0.0076 and 0.0299, respectively, indicating the application potential of the adsorption system. The R_L values between 0 and 1 denote the desired adsorption profile (Pandey and Ravi 2019). The correlation coefficient (R^2) of banana stalks (S), (M), and (L) was 0.9798, 0.9674, and 0.9312, respectively, showing that the small banana stalks (S and M) exhibit a better fit to the Langmuir model than the large banana stalk (L). However, MB adsorption on the large banana stalk (L) did not appear on a monolayer.

The Freundlich isotherm described the heterogeneity of the adsorption system (Pandey and Ravi 2019). The equilibrium data of all sizes of banana stalks (S, M, and L) fitted well to the Freundlich isotherm. The R^2 of banana stalks (S), (M), and (L) was 0.9999, 0.9987, and 0.9994, respectively (Table 1). The R^2 values obtained using the Freundlich model were determined to be greater than those obtained using the Langmuir model. Thus, MB adsorption on various sizes of banana stalks correlated better with the Freundlich model. The results revealed the interaction between MB molecules and different banana stalk surfaces with multilayer adsorption. Notably, the small banana stalk

(S) has the highest R^2 value, with the adsorption capacity of 9.48 mg/g. The inverse adsorption intensity (1/n) of all sizes of banana stalks reflected the favorable process of the adsorption of MB dye on banana stalks (Fytianos et al., 2000). The adsorption pattern of rhodamine B on banana peel was similar to that obtained using the Freundlich model (Oyekanmi et al., 2019).

Agricultural wastes can be used as adsorbents for cationic and anionic dyes. The natural form of agricultural wastes adsorbs cationic dyes better than anionic dyes. Several adsorbents were treated to improve the adsorption capacity for removing anionic dyes (Salleh et al., 2011). In this research, banana stalk waste was used in its natural form. Therefore, carboxylic and hydroxyl groups had a negative charge that enabled the adsorption of cationic dyes, whereas anionic dyes had a negative charge that interfered with the adsorption on the banana stalk surface (Nascimento et al., 2015).

The pH of the solution is one of the factors that affects the dye adsorption of adsorbents in wastewater treatment because of the degree of ionization of the dye molecule and adsorbent surface (Yagub et al., 2014). With the increase in the pH of the solution, cationic dye adsorption on raw pine leaf increased (Yagub et al., 2012). The point of zero charge (pH_{pzc}) was used to describe the electrokinetic properties of the surface. When pH > pH_{pzc}, cationic dye adsorption is favored. By contrast, when pH < pH_{pzc}, the surface becomes positively charged; thus, anionic dye adsorption is favored (Yagub et al., 2014). Cationic dye adsorption occurred at high pH, whereas anionic dye adsorption occurred at low pH (Salleh et al., 2011). This research did not investigate the effect of pH on the household application of this convenient and simple method. When the pH of MB solution is high, the adsorbent surface becomes negatively charged, which increases the adsorption capacity of banana stalk. This finding can be attributed to the generation of electrostatic interaction between the positively charged MB and the negatively charged banana stalk.

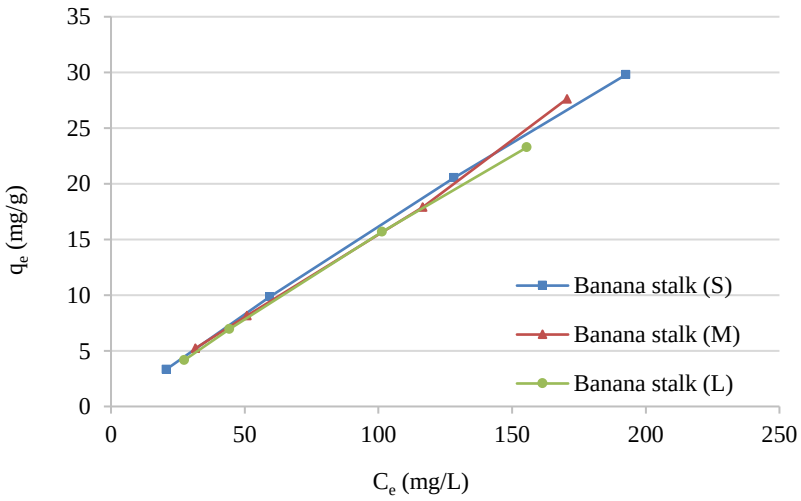

Figure 8 MB adsorption capabilities of various sizes of banana stalks

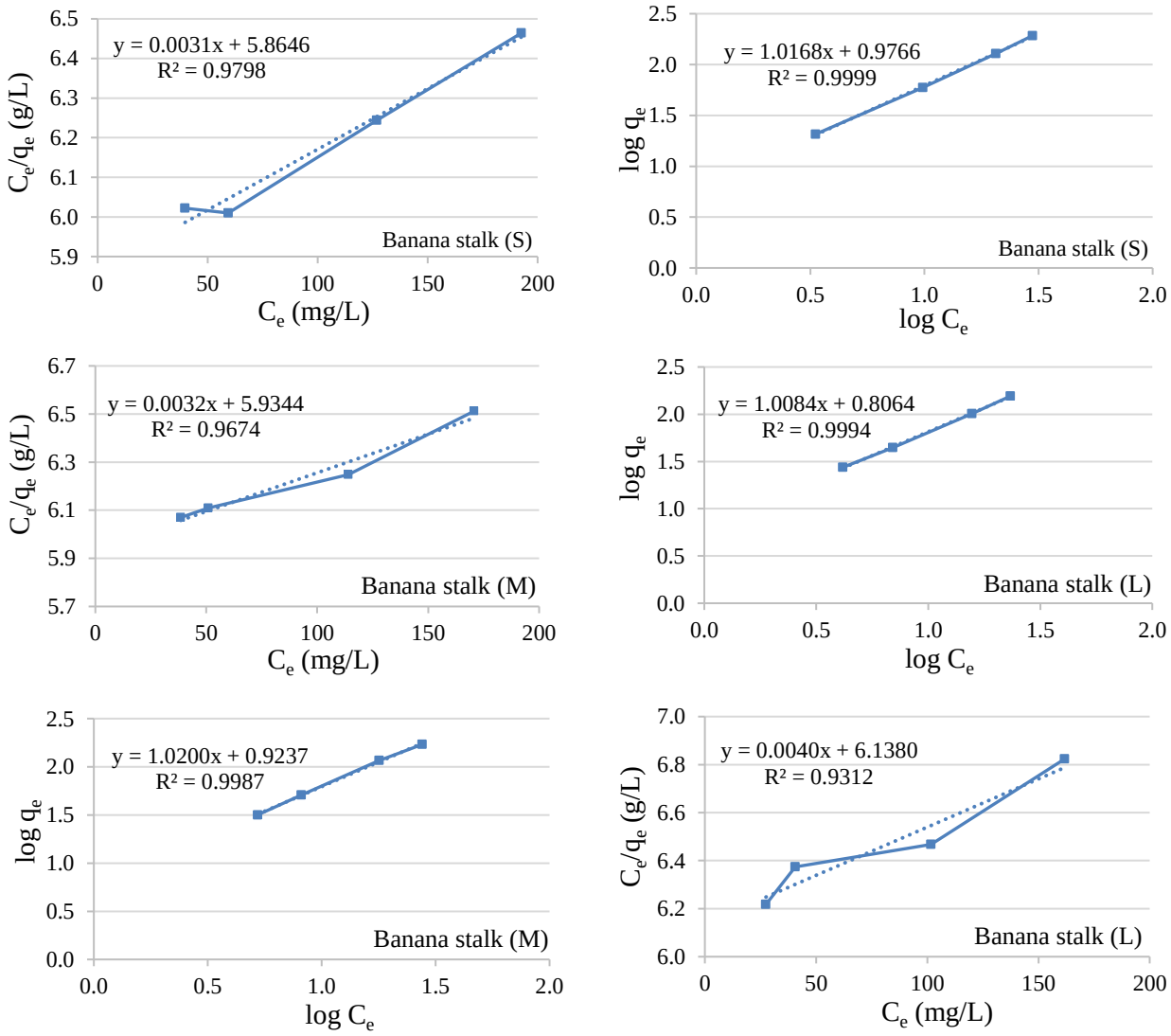

Figure 9 Adsorption isotherms for MB adsorption on various sizes of banana stalks: Langmuir (left) and Freundlich (right) isotherms

Table 1 Parameter values of the Langmuir and Freundlich isotherms for MB adsorption on various sizes of banana stalks

Banana stalk	Langmuir isotherm				Freundlich isotherm		
	K_L (L/mg)	q_m (mg/g)	R_L	R^2	K_F (mg/g)	1/n	R^2
S	0.53	322.58	0.0094 - 0.0364	0.9798	9.48	1.0	0.9999
M	0.54	312.50	0.0092 - 0.0357	0.9674	8.39	1.0	0.9987
L	0.65	250.00	0.0076 - 0.0299	0.9312	6.40	1.0	0.9994

The data were evaluated using two adsorption kinetics models, that is, the pseudo-first-order and pseudo-second-order kinetics models, to predict the mechanism of MB adsorption on various sizes of banana stalks. The pseudo-first-order kinetics model is defined by Lagergren as follows (Ho, 2004):

$$\log (q_e - q_t) = \log q_e - k_1 t/2.303, \quad (6)$$

where q_t and q_e are the adsorption capacities at t and equilibrium, respectively. The plot of $\log (q_e - q_t)$ versus t showed a linear relationship and was used to determine the slopes and intercepts. The k_1 value (min^{-1}) is the pseudo-first-order rate constant and t is the contact time (min).

The pseudo-second-order kinetics model is developed and described as follows (Ho, 2004):

$$t/q_t = 1/k_2 q_e^2 + t/q_e, \quad (7)$$

where k_2 is the pseudo-second-order rate constant. The plot of t/q_t versus t showed a linear relationship. The equilibrium adsorption capacity (q_e) is calculated using 1/slope.

The kinetics parameters for MB adsorption on various sizes of banana stalks are shown in Table 2. The R^2 of banana stalks (S), (M), and (L) for the pseudo-first-order kinetics model was 0.9284, 0.8088, and 0.3786, respectively, which were low and unable to describe the dye adsorption mechanism. By contrast, the R^2 value of banana stalks (S), (M), and (L) for the pseudo-second-order kinetics model was 0.9975, 0.9951, and 0.9435, respectively. These data fitted well to the pseudo-second-order kinetics model. The calculated q_e values for the pseudo-second-order kinetics model of all sizes of banana stalks were quite similar to the experimental values. The pseudo-second-order rate constant (k_2) increased with the decrease in the size of banana stalk, and this model confirmed the chemisorption of MB onto banana stalks. The pseudo-second-order kinetics model generally described dye adsorption as the rate-limiting step, which comprised valence forces that drive the sharing of electrons or exchange of electrons between adsorbent and adsorbate (Mohan et al., 2006; Kula et al., 2008; Zhang et al., 2016).

Table 2 Kinetics parameters for MB adsorption on various sizes of banana stalks

Banana stalk	Pseudo-first-order			Pseudo-second-order			$q_{e,exp}$ (mg/g)
	$q_{e,cal}$ (mg/g)	k_1 (min^{-1})	R^2	$q_{e,cal}$ (mg/g)	k_2 (g mg^{-1} min^{-1})	R^2	
S	13.2801	0.00138	0.9284	10.80	17.55×10^{-3}	0.9975	11.19
M	12.9033	0.00138	0.8088	10.07	12.59×10^{-3}	0.9951	10.68
L	9.6761	0.00230	0.3786	6.32	11.43×10^{-3}	0.9435	6.59

4. CONCLUSION

In this research, banana stalks showed promising adsorption capacity for MB dye in wastewater treatment. Small banana stalks had higher adsorption efficacy than large banana stalks because of the high surface area of the adsorbent. The operating parameters for maximum adsorption were adsorbent amount (0.3 g/50 mL), initial MB dye concentration (150 mg/L), shaking speed (100 rpm), and contact time (60 min). The Freundlich isotherm model was the optimal model for illustrating the adsorption process of all sizes of banana stalks with a high correlation. The most suitable adsorption kinetics

model was the pseudo-second-order kinetics model. Thus, it can be concluded that banana stalk is a suitable adsorbent for MB dye and is an interesting adsorbent for other dyes. Furthermore, the use of banana stalk in the adsorption process is inexpensive and convenient for wastewater treatment in the textile industry.

ACKNOWLEDGMENT

The authors wish to thank the Faculty of Science and Technology and Research and Development Institute, Rajabhat Rajanagarindra University for the facilities and the financial support. The authors acknowledge the Pharmaceutical Intellectual Center "Prachote Plengwittaya", Faculty of Pharmacy, Silpakorn University for providing additional research facilities.

REFERENCES

Amel, K., Hassen, M. A., and Kerroum, D. (2012). Isotherm and kinetics study of biosorption of cationic dye onto banana peel. *Energy Procedia*, 19, 286-295.

Banerjee, S., and Chattopadhyaya, M. C. (2017). Adsorption characteristics for the removal of a toxic dye, tartrazine from aqueous solutions by a low cost agricultural by-product. *Arabian Journal of Chemistry*, 10(2), S1629-S1638.

Becker, H., Matos, R. F., Souza, J. A., Lima, D. A., Souza, F. T. C., and Longhinotti, E. (2013). Pseudo-stem banana fibers: Characterization and chromium removal. *Orbital: Electronic Journal of Chemistry*, 5(3), 164-170.

Bello, O. S., Bello, I. A., and Adegoke, K. A. (2013). Adsorption of dyes using different types of sand: a review. *South African Journal of Chemistry*, 66(1), 117-129.

Bulut, Y., and Aydin, H. (2006). A kinetics and thermodynamics study of methylene blue adsorption on wheat shells. *Desalination*, 194(1-3), 259-267.

Carvalho, H. P., Huang, J., Zhao, M., Liu, G., Dong, L., and Liu, X. (2015). Improvement of methylene blue removal by electrocoagulation/banana peel adsorption coupling in a batch system. *Alexandria Engineering Journal*, 54(3), 777-786.

Danish, M., Ahmad, T., Majeed, S., Ahmad, M., Ziyang, L., Pin, Z., and Iqubal, S. M. S. (2018). Use of banana trunk waste as activated carbon in scavenging methylene blue dye: Kinetic, thermodynamic, and isotherm studies. *Bioresource Technology Reports*, 3, 127-137.

Demirbas, A. (2009). Agricultural based activated carbons for the removal of dyes from aqueous solutions: a review. *Journal of Hazardous Materials*, 167(1-3), 1-9.

Foo, K. Y., and Hameed, B. H. (2010). An overview of dye removal via activated carbon adsorption process. *Desalination and Water Treatment*, 19(1-3), 255-274.

Fytianos, K., Voudrias, E., and Kokkalis, E. (2000). Sorption-desorption behavior of 2,4-dichlorophenol by marine sediments. *Chemosphere*, 40(1), 3-6.

Greluk, M., and Hubicki, Z. (2011). Efficient removal of acid orange 7 dye from water using the strongly basic anion exchange resin amberlite IRA-958. *Desalination*, 278(1-3), 219-226.

Hameed, B. H., Mahmoud, D. K., and Ahmad, A. L. (2008). Sorption equilibrium and kinetics of basic dye from aqueous solution using banana stalk waste. *Journal of Hazardous Materials*, 158(2-3), 499-506.

Ho, Y. S. (2004). Citation review of Lagergren kinetic rate equation on adsorption reactions. *Scientometrics*, 59(1), 171-177.

Kula, I., Ugurlu, M., Karaoglu, H., and Celik A. (2008). Adsorption of Cd(II) ions from aqueous solutions using activated carbon prepared from olive stone by $ZnCl_2$ activation. *Bioresource Technology*, 99(3), 492-501.

Langmuir, I. (1918). The adsorption of gases on plane surfaces of glass, mica and platinum. *Journal of the American Chemical Society*, 40(9), 1361-1403.

Liu, R., Yu, H., and Huang, Y. (2005). Structure and morphology of cellulose in wheat straw. *Cellulose*, 12(1), 25-34.

Mahmoodi, N. M. (2011). Equilibrium, kinetics, and thermodynamics of dye removal using alginate in binary systems. *Journal of Chemical and Engineering Data*, 56(6), 2802-2811.

Manna, S., Roy, D., Saha, P., Gopakumar, D., and Thomas, S. (2017). Rapid methylene blue adsorption using modified lignocellulosic materials. *Process Safety and Environmental Protection*, 107, 346-356.

Mittal, A., Mittal, J., Malviya, A., Kaur, D., and Gupta, V. K. (2010). Adsorption of hazardous dye crystal violet from wastewater by waste materials. *Journal of Colloid and Interface Science*, 343(2), 463-473.

Mohammad, A., Li, J., Salamh, Y., Nasir, A., Walker, G., and Mohammad, N. M. A. (2010). Adsorption mechanisms of removing heavy metals and dyes from aqueous solution using date pits solid adsorbent. *Journal of Hazardous Materials*, 176(1-3), 510-520.

Mohan, D., Singh, K. P., and Singh, V. K. (2006). Trivalent chromium removal from wastewater using low cost activated carbon derived from agricultural waste material and activated carbon fabric cloth. *Journal of Hazardous Materials*, 135(1-3), 280-295.

Moubarak, F., Atmani, R., Maghri, I., Elkouali, M., Talbi, M., and Latifa, M. (2014). Elimination of methylene blue dye with natural adsorbent banana peels powder. *Global Journal of Science Frontier Research: B Chemistry*, 14(1), 39-44.

Mouni, L., Belkhiri, L., Bollinger, J. C., Bouzaza, A., Assadi, A., Tirri, A., Dahmoune, F., Madani, K., and Remini, H. (2018). Removal of methylene blue from aqueous solutions by adsorption on kaolin: kinetic and equilibrium studies. *Applied Clay Science*, 153(1), 38-45.

Nascimento, G. E., Campos, N. F., Silva, J. J., and Marta, D. (2015). Adsorption of anionic dyes from an aqueous solution by banana peel and green coconut mesocarp. *Desalination and water treatment*, 57(30), 14093-14108.

Nujnetra, A., and Boonarong, L. (2013). Kluai Homthong Banlad: (banana production in Banlad) production cost and economic rent. *Advances in Environmental Biology*, 7(9), 2225-2228.

Oyekanmi, A. A., Ahmad, A., Hossain, K., and Rafatullah, M. (2019). Adsorption of rhodamine B dye from aqueous solution onto acid treated banana peel: Response surface methodology, kinetics and isotherm studies. *PLoS ONE*, 14(5), e0216878.

Pandey, L. M., and Ravi, R. (2019). Enhanced adsorption capacity of designed bentonite and alginate beads for the effective removal of methylene blue. *Applied Clay Science*, 169(1), 102-111.

Pathania, D., Sharma, S., and Singh, P. (2017). Removal of methylene blue by adsorption onto activated carbon developed from *Ficus carica* bast. *Arabian Journal of Chemistry*, 10(1), S1445-S1451.

Salleh, M. A. M., Mahmoud, D. K., Karim, W. A. W. A., and Idris, A. (2011). Cationic and anionic dye adsorption by agricultural solid wastes: a comprehensive review. *Desalination*, 280(1-3), 1-13.

Salman, J. M., Njoku, V. O., and Hameed, B. H. (2011). Adsorption of pesticides from aqueous solution onto banana stalk activated carbon. *Chemical Engineering Journal*, 174(1), 41-48.

Sharma, S., Hasan, A., Kumar, N., and Pandey, L. M. (2018). Removal of methylene blue dye from aqueous solution using immobilized *Agrobacterium fabrum* biomass along with iron

oxide nanoparticles as biosorbent. *Environmental Science and Pollution Research*, 25(22), 21605-21615.

Shimizu, F. L., Monteiro, P. Q., Ghiraldi, P. H. C., Melati, R. B., Pagnocca, F. C., Souza, W., Anna, C. S., and Brienzo, M. (2018). Acid, alkali and peroxide pretreatments increase the cellulose accessibility and glucose yield of banana pseudostem. *Industrial Crops and Products*, 115, 62-68.

Singh, S., Parveen, N., and Gupta, H. (2018). Adsorptive decontamination of rhodamine-B from water using banana peel powder: a biosorbent. *Environmental Technology & Innovation*, 12, 189-195.

Sulak, M. T., Demirbas, E., and Kobya, M. (2007). Removal of astrazon yellow 7GL from aqueous solutions by adsorption onto wheat bran. *Bioresource Technology*, 98(3), 2590-2598.

Vadivelan, V., and Kumar, K. V. (2005). Equilibrium, kinetics, mechanism, and process design for the sorption of methylene blue onto rice husk. *Journal of Colloid and Interface Science*, 286(1), 90-100.

Vital, R. K., Saibaba, K. V. N., Shaik, K. B., and Gopinath, R. (2016). Dye removal by adsorption: a review. *Journal of Bioremediation Biodegradation*, 7(6), 371.

Xie, K., Zhao, W., and He, X. (2011). Adsorption properties of nano-cellulose hybrid containing polyhedral oligomeric silsesquioxane and removal of reactive dyes from aqueous solution. *Carbohydrate Polymers*, 83(4), 1516-1520.

Yagub, M. T., Sen, T. K., and Ang, H. M. (2012). Equilibrium, kinetics, and thermodynamics of methylene blue adsorption by pine tree leaves. *Water Air & Soil Pollution*, 223(8), 5267-5282.

Yagub, M. T., Sen, T. K., Afroze, S., and Ang, H. M. (2014). Dye and its removal from aqueous solution by adsorption: a review. *Advances in Colloid and Interface Science*, 209, 172-184.

Zhang, S., Wang, Z., Zhang, Y., Pan, H., and Tao, L. (2016). Adsorption of methylene blue on organosolv lignin from rice straw. *Procedia Environmental Sciences*, 31, 3-11.

Zhao, B., Xiao, W., Shang, Y., Zhu, H., and Han, R. (2017). Adsorption of light green anionic dye using cationic surfactant-modified peanut husk in batch mode. *Arabian Journal of Chemistry*, 10(2), S3595-S3602.